Journal of Physics: Conference Series **736** (2016) 012010 doi:10.1088/1742-6596/736/1/012010

Latest Heavy Flavor Results from the PHENIX Experiment at RHIC

Alexandre Lebedev for the PHENIX Collaboartion
Department of Physics and Astronomy, Iowa State University, Ames, IA 50011-3160, USA
E-mail: lebedev@iastate.edu

Abstract. Heavy quark production can be used as a stringent test of perturbative QCD in proton-proton collisions, and is a valuable reference for the study of heavy ion collisions. In nucleus-nucleus collisions, the measurement of heavy quark production provides a powerful tool for studying the properties of hot and dense matter created in these collisions. The PHENIX experiment has studied many important observables related to heavy flavor via leptonic measurements. Such observables include the invariant yield and azimuthal anisotropy of electrons from non-photonic sources and prompt single muons, both of which are dominated by decays of D and B mesons. Complimentary to single lepton measurements, PHENIX has measured invariant yield, flow, and polarization of various quarkonia states. Such measurements provide additional insight into heavy flavor production mechanisms. The most recent PHENIX heavy flavor results will be presented, and compared to various theoretical model predictions.

1. $\psi(2S)/J/\psi$ ratios in p+Au and p+Al collisions

The PHENIX experiment has measured previously [1] $\psi(2S)$ nuclear modification factor in d+Au collisions at $\sqrt{s} = 200$ GeV/c. The measurement was done at mid-rapidity. The magnitude and the trend with centraility of $\psi(2S)$ meson suppression turned out to be very different than that of J/ψ [2]. In most central d+Au collisions $\psi(2S)$ suppression was measured to be almost 3 times larger than that of J/ψ. Since the initial state factors in a nucleus, such as shadowing and energy loss, should be the same or very similar for $c\bar{c}$ precursor pairs for both $\psi(2S)$ and J/ψ, something different must be happening in the later stages of the collision.

The new PHENIX measurement of $\psi(2S)$ production in p+p, p+Au and p+Al collisions at $\sqrt{s} = 200$ GeV/c at forward/bacward rapidity may shed light on the relatively large suppression of $\psi(2S)$. Fig. 1 shows the fraction of $\psi(2S)/J/\psi$ as a function of transverse momentum (p_T) in proton-proton collisions. Integrated over all p_T, this fraction is around 2%, which is in agreement with the world data (see Fig. 2). This measurement serves as a baseline for the proton-nucleus measurements.

Fig. 3 shows relative suppression of $\psi(2S)/J/\psi$ as a function of rapidity for p+Au and p+Al collisions, as well as the old d+Au result at mid-rapidity. In the proton-going direction (positive rapidity) suppression of $\psi(2S)$ is, essentially, the same as that of J/ψ, while in the nucleus-going direction (negative rapidity) $\psi(2S)$ are much more suppressed both in p+Au and p+Al collisions. In other words, $\psi(2S)$'s are strongly suppressed in both directions, while J/ψ's are strongly suppressed in proton-going direction, and moderately in nucleus-going direction.

Fig. 4 shows relative suppression of $\psi(2S)/J/\psi$ as a function of transverse momentum. As one can see, the slowest J/ψ, which spend the most time with soft co-movers are completely

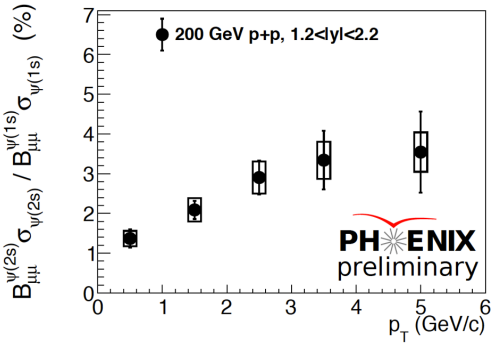

Figure 1. Fraction of $\psi(2S)/J/\psi$ as a function of transverse momentum in proton-proton collisions.

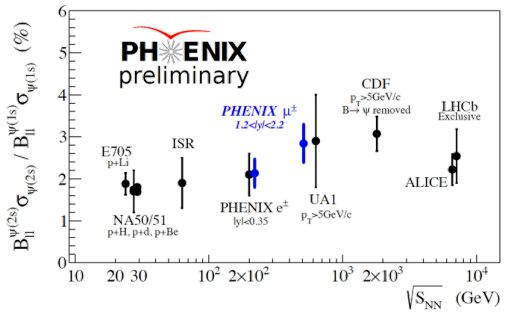

Figure 2. Integrated over p_T $\psi(2S)/J/\psi$ fraction as a function of $\sqrt{s}$.

gone. Thus looks qualitatively different from similar results from the ALICE experiment [9], where little or no dependence on J/ψ transverse momentum is observed. However, both results agree within rather large experimental uncertainties.

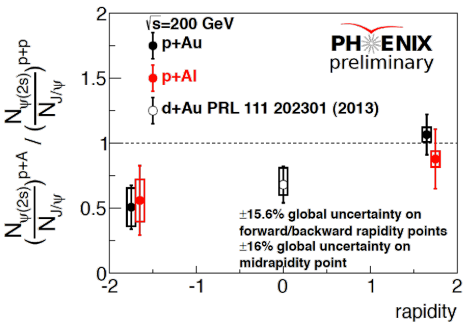

Figure 3. Relative $\psi(2S)/J/\psi$ suppression as a function of rapidity.

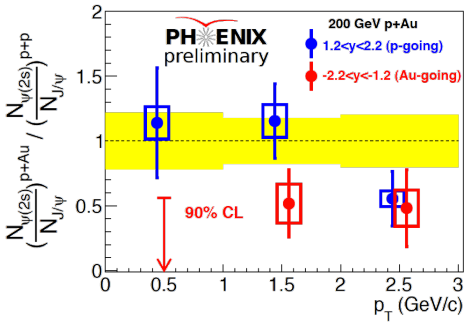

Figure 4. Relative $\psi(2S)/J/\psi$ suppression as a function of transverse momentum.

2. J/ψ suppression in U+U collisions

J/ψ suppression at RHIC energies is much stronger than that at LHC energies for similar energy density created in nucleus-nucleus collisions, which may be an indication of importance of coalescence at LHC. At the same time, at RHIC, J/ψ suppression is almost the same at $\sqrt{s}$ = 39, 62 and 200 GeV, perhaps being strongest at 200 GeV. It can be explained as a balance between color screening and coalescence [3]. So, the question is, when does the coalescence becomes important? Colliding uranium nuclei allows us to go to higher energy density at RHIC and, perhaps, answer this question. Central U+U collisions are expected to have 15-20% higher energy density than central Au+Au collisions, and increased charm production from larger (by ~25%) number of binary collisions (N_{coll}). The former will make color screening stronger, while the latter will result in more coalescence.

The calculation of number of binary collisions for the uranium-uranium collisions is complicated by the non-spheric shape of the uranium nucleus. In this study we used two different shapes. The first one is a "conventional" description of the uranium nucleus

deformation, where the mean radius and diffuseness are taken from electron scattering measurements [7]. The second parametrization [8] takes into account the finite radius of a nucleon and averages over all orientations of axis-of-symmetry. Average radius and diffuseness obtained from this parametrization matches values from electron scattering measurements. The first parametrization has larger surface diffuseness, which results in a less compact nucleus, larger cross-section (by ∼12%), and smaller number of binary collisions (by 6-15%).

Figs. 5 and 6 show J/ψ nuclear modification factor (R_{AA}) in uranium-uranium collisions as a function of number of participant nucleons for the first and second parametrizations. On the same figures R_{AA} for Au+Au collisions is shown for comparison. In both cases in most central events J/ψ suppression in U+U collisions appears to be less strong than that in Au+Au collisions.

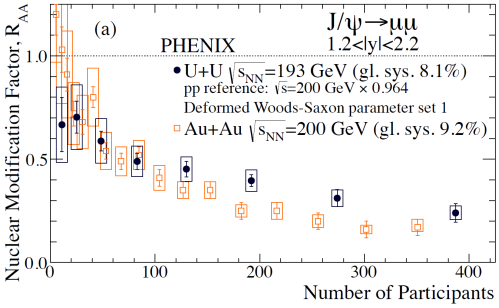

Figure 5. $J\psi$ nuclear modification factor R_{AA} as a function of number of participant nucleons for the first parametrization.

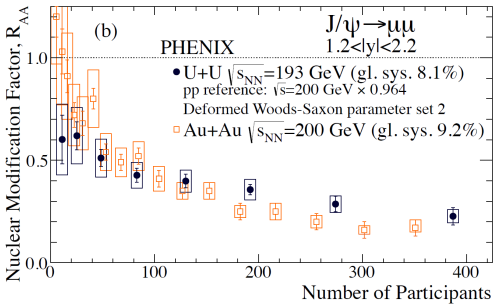

Figure 6. $J\psi$ nuclear modification factor R_{AA} as a function of number of participant nucleons for the second parametrization.

The measured U+U/Au+Au ratio vs. centrality does not depend on number of binary collisions. However, we can predict how this ratio would change if J/ψ production is only dependent on N_{coll}. Fig. 7 shows experimentally measured J/ψ R_{AA} ratio in U+U and Au+Au collisions as a function of centrality. Color curves in this fiigure show how the ratio should change if J/ψ production scales with N_{coll} (dashed curves) or N^2_{coll} (solid curves). The first parametrization favors N^2_{coll} dependence, while the first one is consistent with both N^2_{coll} and N_{coll}, slightly favoring the former in most central collisions. This observation is consistent with the picture in which the increase in charm coalescence becomes more important than the increased color screening when going from Au+Au to U+U collisions.

3. $b\bar{b}$ production in p+p collisions

3.1. Opposite sign di-electrons at $\sqrt{s} = 200$ *GeV*

Beauty production in p+p collisions at $\sqrt{s} = 200$ GeV was studied using opposite sign di-electrons using simultaneous fit of invariant mass and transverse momentum distributions [4].

The spectrum of di-electrons produced in p+p collisions is well understood in terms of hadronic cocktail (at low mass) and Drell-Yan, charm, and beauty decays (high mass). After the yield from vector and pseudo-scalar mesons, and Drell-Yan is subtracted from the measured di-electron spectrum, we are left with di-elctrons from semi-leptonic decays of charm and beauty. The main idea behind charm/beauty separation is that di-electrons from charm dominate low invariant mass and low p_T region of this two-dimasional space, while di-electrons from beauty dominate either high mass and low p_T, or low mass and high p_T regions. One-dimensional projections of two-dimensional fits to invariant mass axis are shown in Fig. 8.

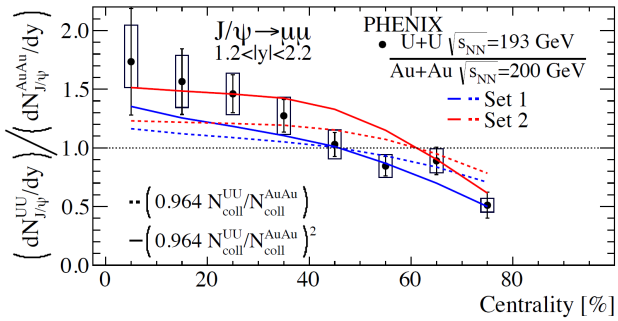

Figure 7. Measured ratio of J/ψ nuclear modification factors in U+U and Au+Au collisions as a function of centrality. Blue curves: first parametrization; red curves: second parametrization. Dashed curves: N_{coll} dependence; solid curves: N_{coll}^2 dependence.

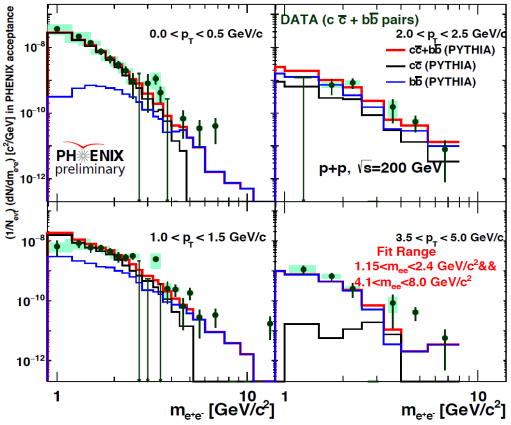

Figure 8. Invariant mass distributions of opposite sign electron pairs after subtraction of the yield from vector and pseudo-scalar mesons, and Drell-Yan in four p_T bins. Black: $c\bar{c}$ yield, blue: $b\bar{b}$ yield, red: the sum.

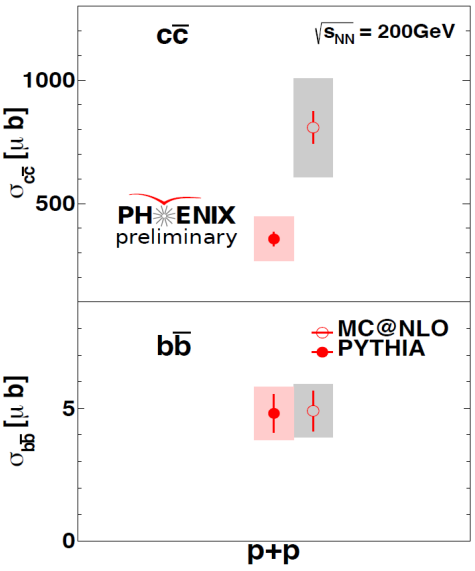

Figure 9. Integrated $c\bar{c}$ (top) and $b\bar{b}$ (bottom) cross-section obtained using PYTHIA and MC@NLO models.

This approach is model-dependent, since the decay electron spectra depend on original charm/beauty distributions. However, for heavier quarks (beauty) the effect of the original quark distribution gets smeared by the decay kinematics, and the results do not depend on the chosen model. This is not true in case of charm. We used two models, tuned PYTHIA [5] and MC@NLO in this study [6]. The integrated $c\bar{c}$ and $b\bar{b}$ cross-section obtained in this way is shown in Fig. 9. The $b\bar{b}$ cross-section shows, as expected, no model dependence, while $c\bar{c}$ cross-section is strongly dependent on rapidity shape of the original quark distribution, which is different in PYTHIA and MC@NLO.

3.2. Same sign dimuons at $\sqrt{s} = 510$ GeV

Another way of separating charm and beauty contributions to di-lepton spectra is to use same sign di-leptons (muons in this case). This approach is based on B-meson oscillations. The

advantage of this method is that it has very low background. There is no contamination from Drell-Yan, quarkonia, or vector mesons.

The spectrum of same sign dimuons consistes of combinatorial background (calculated using mixed events method), and correlated pairs. The correlated same sign pairs contain, in addition to the signal, contribution from charm pairs (negligible in PHENIX acceptance), and the background from jets. This last contribution is the major source of the experimental uncertainty, and is calculated using hadronic simulations.

Fig. 10 shows invariant mass distribution of same sign dimuons measured in p+p collisions at $\sqrt{s} = 510$ GeV after combinatorial background subtraction at backward (top) and forward (bottom) rapidity. The difference between top and bottom plots is due to the fact that the amount of material in front of the PHENIX South and North Muon Arms is very different, resulting in different hadronic contamination.

Total $b\bar{b}$ integrated cross-section is shown in Fig. 11. The integration of cross-section to lower invariant masses is done using PYTHIA. This $b\bar{b}$ cross-section is slightly above the one predicted by NLO pQCD [10], but the two agree within experimental and theoretical uncertainties.

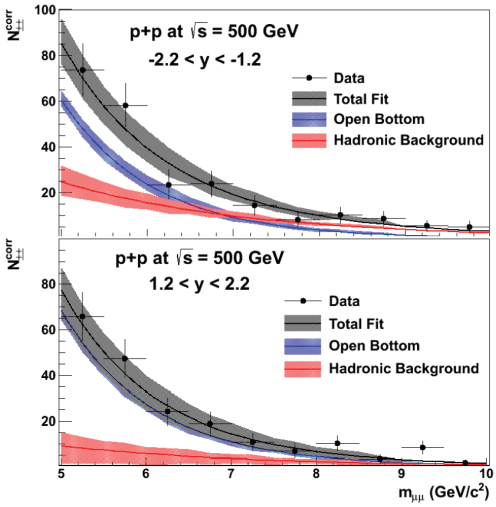

Figure 10. Invariant mass distributions of same sign muon pairs after subtraction of combinatorial background. The difference between the top and bottom plots is due to different amount of material in front of the PHENIX South and North muon arms.

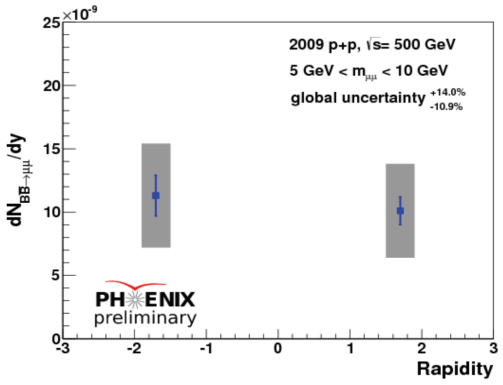

Figure 11. Total $b\bar{b}$ integrated cross-section as a function of rapidity.

4. Summary

We have reviewed recent quarkonia results from the PHENIX experiment at RHIC.

In proton-nucleus collisions $\psi(2S)$ suppression is larger than that of J/ψ in nucleus-going direction, and the same in proton-going direction. Qualitatively, this observation is unlike what was observed at LHC energies, but the difference is within experimental uncertainty. Very strong $\psi(2S)$ suppression is observed at low transverse momentum.

In U+U collisions, J/ψ suppression is weaker than in Au+Au collisions. This is consistent with dominance of coalescence over color screening. Centrality dependence of U+U/Au+Au ratio of nuclear modification factors is also consistent with the importance of coalescence.

PHENIX measured $b\bar{b}$ production using opposite sign electrons at $\sqrt{s} = 200$ GeV, and same sign muons at $\sqrt{s} = 510$ GeV. Both results are somewhat higher than NLO pQCD calculation, but agree with it within uncertainty.

References

[1] A. Adare et al., (PHENIX Collaboration) Phys. Rev. Lett. **111**, 202301 (2013)
[2] A. Adare et al., (PHENIX Collaboration) Phys. Rev. Lett. **107**, 142301 (2013)
[3] X. Zhao and R.Rapp, Phys. Rev. C **82**, 064905 (2010)
[4] A. Adare et al., (PHENIX Collaboration) Phys. Rev. C **91**, 014907 (2015)
[5] T. Sjostrand, S. Mrenna, and P. Z. Skands, J. High Energy Phys. **5**, 026 (2006)
[6] S. Frixione and B. Webber, J. High Energy Phys. **6**, 029 (2002)
[7] H. Masui, B. Mohanty, and N. Xu, Phys. Lett. B **679**, 440 (2009)
[8] Q. Y. Show et al., Phys. Lett. B **749**, 215 (2015)
[9] B. Abelev et al., (ALICE Collaboration) J. High Energy Phys. (2014) 2014:73, doi:10,1007/JHEP12(2014)073
[10] R. Vogt, Eur.Phys.J.ST 155:213-222.2008, arXiv:0709.2531v1